Advantages and pitfalls of noninvasive electrocardiographic imaging

Laura R. Bear, Oumayma Bouhamama, Matthijs Cluitmans, Josselin Duchateau, Richard D. Walton, Emma Abell, Charly Belterman, Michel Haissaguerre, Olivier Bernus, Ruben Coronel, et al.

HAL Id: hal-03488455

https://hal.science/hal-03488455

Submitted on 21 Dec 2021

1   **"Advantages and pitfalls of noninvasive electrocardiographic imaging"**

2   *Laura R Bear, PhD[1,2,3], Oumayma Bouhamama, MSc[1,2,3,4], Matthijs Cluitmans, PhD, MD[5],

3   Josselin Duchateau, PhD[1,2,3,6], Richard D Walton, PhD[1,2,3], Emma Abell, MSc[1,2,3],

4   Charly Belterman, Msc[1,7], Michel Haissaguerre, PhD, MD[1,2,3,6], Olivier Bernus, PhD[1,2,3],

5   Ruben Coronel, PhD, MD[1,7], Rémi Dubois, PhD[1,2,3]

6   1 IHU Liryc, Electrophysiology and Heart Modeling Institute, fondation Bordeaux Université, F-33600

7   Pessac- Bordeaux, France

8   2 Université de Bordeaux, Centre de recherche Cardio-Thoracique de Bordeaux, U1045, F-33000,

9   Bordeaux, France

10   3 INSERM, Centre de recherche Cardio-Thoracique de Bordeaux, U1045, F-33000 Bordeaux, France

11   4 INRIA

12   5 CARIM School for Cardiovascular Diseases, Maastricht UMC, Maastricht, Netherlands

13   6 Bordeaux University Hospital (CHU), Electrophysiology and Ablation Unit, F-33600 Pessac, France

14   7 Department of Experimental Cardiology, Academic Medical Center, the Netherlands

15

16

17

18

19

20   *Dr Laura Bear

21   IHU-LIRYC, Site Xavier Arnozan, Avenue du Haut Lévêque, 33600 Pessac, France

22   laura.bear@ihu-liryc.fr

23   +33(0) 535 38 1967

24

1 **Abstract (250 word limit)**

2 **Background:** With increasing clinical use of Electrocardiographic Imaging (ECGI), it is imperative to

3 understand the limits of this technique. The objective of this study is to evaluate a potential-based

4 ECGI approach for activation and repolarization mapping in sinus rhythm.

5 **Method:** Langendorff-perfused pig hearts were suspended in a human-shaped torso tank.

6 Electrograms were recorded with a 108-electrode sock and ECGs with 256 electrodes embedded in

7 the tank surface. Left bundle branch block (LBBB) was developed in 4 hearts through ablation, and

8 repolarization abnormalities in another 4 hearts through regional perfusion of dofetilide and

9 pinacidil. Electrograms were noninvasively reconstructed and reconstructed activation and

10 repolarization features were compared to those recorded.

11 **Results:** Visual consistency between ECGI and recorded activation and repolarization maps was high.

12 While reconstructed repolarization times showed significantly more error than activation times

13 quantitatively, patterns were reconstructed with a similar level of accuracy. The number of epicardial

14 breakthrough sites was underestimated by ECGI and these were misplaced (>20 mm) in location.

15 Likewise, ECGI reconstructed activation maps demonstrated artificial lines of block resulting from a

16 W-shaped QRS waveform that were not present in recorded maps. Nevertheless, ECGI allowed

17 identification of regions of abnormal repolarization reasonably accurately in terms of size, location

18 and timing.

19 **Conclusions:** This study validates a potential-based ECGI approach to noninvasively image activation

20 and recovery in sinus rhythm. Despite inaccuracies in epicardial breakthroughs and lines of

21 conduction block, other important clinical features such as regions of abnormal repolarization can be

22 accurately derived making ECGI a valuable clinical tool.

23 **Keywords:** Non-invasive Electrocardiography; Torso Tank; Activation; Repolarization;

1   Introduction

2   Electrocardiographic imaging (ECGI) is a non-invasive tool that can be used to panoramically

3   image epicardial cardiac electrical activity using densely sampled body surface potentials and a

4   patient-specific torso model. This technique is being used clinically to reveal electrophysiological

5   substrates in patients with electrical diseases such as abnormally located epicardial breakthroughs,

6   lines of conduction block and regions of delayed depolarization or abnormal repolarization [1–3].

7   These ECGI reconstructed features could provide the basis for alternative risk-stratification

8   techniques.

9   In order for this goal to be realized, the reconstructed activation and repolarization maps and

10   the abnormal features identified must be accurate representations of the true electrical

11   abnormalities in these diseased patients. In a recent clinical study the accuracy of an epicardial

12   potential-based ECGI approach has been investigated for the first time during sinus rhythm [4]. By

13   comparing ECGI reconstructions to epicardial electro-anatomic mapping, several inaccuracies in ECGI

14   maps were highlighted in that study. These included inaccuracies in the position and length of lines

15   of conduction block and the underrepresentation and inaccurate localization of epicardial

16   breakthrough sites (76 ± 37 mm).

17   These results put into question the accuracy of the electrophysiological substrates that have

18   been previously identified using the same ECGI system in patients, including repolarization

19   abnormalities where validation has not yet been performed. Furthermore the source of these

20   inaccuracies during activation has yet to be determined. The question is whether these are due to 1)

21   the ECGI inverse method itself, 2) the feature extraction methods, or 3) other sources of error (such

22   as respiration movement, torso inhomogeneities, error in sequential activation mapping, or

23   alignment of the ECGI with electro-anatomic geometries).

24   Many previous validation studies using epicardial potential based ECGI methods have been

25   performed using experimental data from perfused large animal hearts suspended in human shaped

26   torso tanks [5,6]. These set ups overcome the limitations of clinical validation: being devoid of

respiration movement and having the ability to panoramically map the gold-standard epicardial electrical activity mapped to the same geometry. In this manner one can evaluate the efficacy of ECGI inverse and post-processing methods, understand the source of any inaccuracies and develop new methods to overcome them.

In this study, we aim to evaluate the efficacy of an epicardial potential based ECGI approach to reconstruct activation and repolarization maps and their features using a torso tank experimental model.

Materials and Methods

A subset of the experimental data will be made available for the electrocardiographic imaging community, through the EDGAR project (http://www.ecg-imaging.org/), a collaborative effort by the Consortium for ECG Imaging. The analytic methods used are not included as there are open-source applications that are already widely available.

Torso Tank Experimental Setup

The experimental protocol was approved by Directive 2010/63/EU of the European Parliament on the protection of animals used for scientific purposes and the local ethical committee and has previously been described in [7]. Briefly, hearts were excised from pigs (n = 8; 30–40 kg) and perfused in Langendorff mode with a Tyrode's solution, oxygenated with 95%/5% O_2/CO_2 (pH 7.4, 37°C). An electrode sock (108 electrodes) covering the epicardial surface of the heart was attached to the ventricles. After instrumentation, the heart was transferred to a human-shaped torso tank with 256 electrodes embedded in the surface. In 4 hearts (Group 1), left bundle branch block (LBBB) was induced by radiofrequency ablation. In another 4 hearts (Group 2), regional repolarization heterogeneities were introduced through perfusion of Dofetilide (250 nM) into the non-LAD coronaries and subsequently Pinacidil (30 uM) into the left anterior descending (LAD) artery. For both groups, tank and sock potentials were recorded simultaneously (BioSemi, the Netherlands) during sinus rhythm. These recordings were taken after ablation for Group 1, and before and after the two

drug interventions for Group 2. After each experiment, a 3D fluoroscopic scan (Artis, Siemens) was used to obtain the position of the epicardium, coronaries and electrodes with respect to the tank.

Signal Processing and Inverse Reconstruction

Tank and sock channels in which signals were absent or of poor quality on visual inspection were discarded. A multi-lead signal averaging algorithm was used to remove high-frequency noise in the recordings to produce one beat for each activation sequence in each heart [8]. In total, 8 activation sequences (4 from group 1 hearts and 4 from group 2 hearts in control), and 12 recovery sequences (from group 2 hearts in control and the 2 drug interventions).

ECGI electrograms were reconstructed from the torso tank potentials to experiment-specific epicardial surfaces using the Method of Fundamental Solutions [6] with Tikhonov zero-order regularization [9] and the CRESO method [10] to define the regularization parameter. For each experiment, the sock electrode positions and the epicardial surfaces were constructed from the 3D fluoroscopic scans using Seg3D [11].

Activation times were defined from recorded sock and ECGI electrograms as the time of minimum derivative (dV/dt) over the QRS. Recovery times were defined from recorded sock and ECGI-derived electrograms as the time of maximum dV/dt of the T-wave [12]. A spatio-temporal algorithm developed to define activation times from ECGI electrograms [13] was also investigated for both activation and repolarization. A spatial median filter with 15 mm radius was performed on both recorded and ECGI repolarization times. The 15 mm radius was used as this was found to be the optimal distance to preserve the regions of abnormality in recorded maps, while removing obvious outliers in an automated fashion.

Comparisons and Statistical Analysis

ECGI and sock derived activation and recovery maps were directly compared using the mean absolute error (MAE) and Pearson's correlation coefficient (CC).

The following features of the activation and recovery maps were also quantified and compared. Epicardial breakthrough sites were defined manually from activation maps in hearts in group 2, using the criteria of being a site with an activation time earlier than all surrounding electrodes. When activation was near simultaneous at neighboring electrodes or nodes , the center of the area with <10 ms difference in AT was taken as the breakthrough site. For each activation map, we compared the number of breakthroughs identified using each modality. We also calculate the Euclidean distance and difference in timing between the ECGI-detected and the nearest recorded breakthroughs.

Lines of conduction block were automatically computed from activation maps from hearts in groups 1 and 2 as a jump in the local activation time of 50 ms or more between adjacent electrodes as previously described [14]

Regions of abnormal recovery from hearts in group 2 were defined as repolarization times outside the normal range of repolarization as defined from sock recordings in control state (no drugs) over all hearts at a cycle length of 600 ms (earlier than 180 ms or later than 310 ms). ECGI and recorded abnormally early and late regions were compared in terms of the mean time in the region, the size of the abnormal region, and the localization error of the center of these regions (defined by the Euclidean offset).

Statistical analysis was conducted using GraphPad Prism 7.04. For each metric, the significance of differences was tested using paired t-tests with $p < 0.05$ defined as significant. Relationship between variables was evaluated using a Pearson's Correlation. Data are expressed as mean ± SD unless otherwise stated.

Results

Activation and Recovery Mapping

Figures 1 and 3 show examples of recorded and ECGI reconstructed activation and repolarization maps, with numerical comparison in Table 1. Qualitative consistency between ECGI

and recorded maps was high. The MAE for activations maps was moderately correlated to the QRS duration ($R^2 = 0.54$; p = 0.01), but there was no correspondence between CC and QRS duration ($R^2 = 0.09$; p = 0.69). This suggests that the slower activation sequences will demonstrate bigger errors in timing, but that the activation pathway itself is as accurate as with fast activation sequences.

The CC for repolarization maps were not significantly different from those for activation maps using the dV/dT, although the MAE of activation was significantly smaller than that of repolarization (p<0.05). As with activation, the MAE of repolarization was moderately correlated to the T-wave interval ($R^2 = 0.43$; p=0.02) but not the CC ($R^2 = 0.19$; p = 0.31).

Using a spatio-temporal approach to compute the activation marker placement significantly improved CC and MAE (p<0.001), but produced less accurate results for repolarization marker placement.

Epicardial Breakthroughs

Figure 1A and B present two examples of recorded (left) and ECGI (right) reconstructed activation maps in normal sinus rhythm with epicardial breakthrough sites marked in yellow (recorded) and grey (ECGI). Table 2 summarizes the numerical comparisons of epicardial breakthrough sites. ECGI tends to smooth over the early activation regions, blending neighboring individual breakthroughs into a large region with very similar activation times. ECGI underestimated the number of epicardial breakthrough sites compared to recorded maps (2.6 ± 0.9 v 1.1 ± 0.3). The breakthrough sites that were captured were substantially shifted in location relative to the nearest recorded breakthrough site. The timing of the ECGI breakthrough sites were similar to the true breakthrough sites (Table 2).

Line of Block

Figure 2A presents example activation maps in hearts with LBBB showing (left) smooth propagation of recorded activation (left). The reconstructed activation map using the min dVdT

1   method (middle) demonstrates a long line of block across the septum between the ventricles. Across

2   all recorded activation maps, lines of block were not present in either normal sinus rhythm nor in the

3   presence of LBBB. However, lines of block were present in 4 of the 8 ECGI reconstructed activation

4   maps using the min dVdT as the activation time marker. This only occurred in hearts with LBBB when

5   QRS duration was longer (Figure 2D). Using a spatio-temporal approach (right) helped to smooth the

6   activation maps (right) but did not completely remove the region of slowed conduction. This method

7   removed 3 of the 4 artificial lines of blocks across the 8 maps.

8   Recorded electrograms over the septum (Figure 2B) demonstrate a smooth transition of the

9   intrinsic deflection from early to late activation (initially negative to initially positive QRS). For ECGI

10   electrograms (Figure 2C), the intrinsic deflection also shows this transition, but the electrogram is not

11   accurately reconstructed at the artificial line of block with an initial down-stroke before the R-wave.

12   On the right ventricle, activation is detected on the first downstroke (green electrogram) and shows a

13   sudden transition to the second down-stroke on the left ventricle (cyan electrogram), resulting in the

14   artificial line of block. The spatiotemporal approach considers the delays between electrograms as

15   well as the minimum derivative which helps reduce these artificial jumps in activation time.

16   Regions of Recovery Abnormality

17   Figure 3a and 3b present examples of repolarization maps during normal sinus rhythm (3a) in control

18   and (3b) in the presence of regional Pinacidil and Doftelide perfusion through the LAD (black) and

19   non-LAD coronaries, respectively. Qualitative consistency between the early and late repolarization

20   regions of the heart was high. To quantify this, regions of late and early recovery were marked as

21   repolarization times >310 ms and <180 ms. Numerical comparison of early and late recovery areas is

22   presented in Table 2

23   ECGI correctly identified the presence or absence of early and late recovery regions in all

24   cases. The timing of these regions and the location of the center of these regions were accurately

25   captured with no difference between early or late regions (p = 0.73). ECGI significantly overestimated

1   the size of the early regions (p = 0.02) and underestimated the size of late regions (p = 0.007) by <1

2   cm^2 (both early and late).

3   Discussion

4   In this study we have demonstrated that an epicardial potential based ECGI can be used to

5   reconstruct the general pattern of activation and repolarizations maps in sinus rhythm (normal, LBBB

6   or with repolarization abnormalities) with reasonable accuracy. While some features are accurately

7   captured, others are inaccurate, missing or artificial.

8   First, during sinus rhythm several epicardial breakthrough sites were missing from ECGI maps

9   compared to those recorded, although they were correct in timing. ECGI also demonstrated to be

10   substantially less accurate at localizing epicardial breakthroughs than at localizing PVC or pacing

11   locations at <5 mm in a torso tank [5,6]. Results are mostly consistent with clinical validation [4],

12   except in terms of localization error which was substantially lower in the tank than that seen in

13   patients. This is likely due to respiratory movement of the hearts with the torso compounding

14   localization error clinically (>2 cm in some cases), or the size of the human compared to the pig

15   hearts making it possible for much larger shifts in epicardial breakthroughs. Given that abnormal

16   breakthrough sites have been previously pointed to as potential causal mechanisms of arrhythmia or

17   as markers of disease progression with ECGI [3], it is important to take these results into account for

18   diagnostic purposes. Other methods to define epicardial breakthrough sites, such as through

19   potential maps or by the shape of the RS portion of the electrograms, may prove more accurate with

20   ECGI reconstructions.

21   In this study, lines of conduction block were present in some (but not all) ECGI derived activation

22   maps and was absent from all recorded maps. These lines of block were identified only in the

23   presence of LBBB when the QRS duration was long, consistent with validation in a clinical setting [4].

24   From analysis of ECGI reconstructed electrograms, it can be seen that this phenomenon arises due to

25   an inaccuracy in the reconstruction electrograms demonstrating a W-shape during the mid-activation

26   phase. Using the min dV/dt method, activation marker placement jumps from the first down-stroke

to the second over a small area creating an artificial line of block. We suspect the W-shaped electrograms arise as the reconstructed potentials do not truly represent local epicardial activation but rather a far-field representation of both the epicardial and endocardial electrical activity. This can be seen by the lack of a sharp intrinsic deflection in the ECGI reconstructed electrograms, and the more smooth appearance. This probably has the largest effect on the epicardial regions over the septal region, where indeed the lines of conduction block were usually localized. With further analysis, it may be possible to develop new activation marker placement methods to overcome this limitation and more accurately define epicardial activation times. Indeed, other spatio-temporal activation mapping methods for ECGI do exist that may improve results [15,16]. Furthermore, if the artificial lines of block cannot be eliminated, there are likely other features that can be extracted to differentiate slowed from normal activation such as regions of abnormally late activation or interventricular dyssynchrony (a feature that we have previously demonstrated is accurately reconstructed with the same ECGI approach [7]).

Overall, ECGI reconstructs repolarization as accurately as activation in sinus rhythm when using the dV/dt method to compute markers. While MAE was larger with repolarization, this reflects the larger dispersion of repolarization rather than better accuracy of activation patterns, with both activation and repolarization MAE being correlated to QRS and T-wave intervals, respectively. Unlike with activation, the spatio-temporal approach produced substantially less accurate results with repolarization times. This is unsurprising as the method is based on measuring the delay between neighboring electrograms reflecting activation wave-front propagation, a spatial-connection that does not necessarily exist in repolarization. However, there are many alternative methods available, or that could be developed to define repolarization times that could improve the accuracy of ECGI for mapping recovery. Nevertheless, the derivative approach does allow accurate reconstruction of the location and timing of abnormal recovery regions, and therefore presents a potentially important feature to stratify patients at risk of arrhythmia [2].

This work should be considered in light of the limitations inherent in the study. Namely, this study considers only one implementation for solving the inverse problem of electrocardiography. While this particular epicardial potential based approach is one of the more common methods, there exist a multitude of other methods to not only to describe the cardiac source [17–19], but also to define the forward model [20,21], solve for the regularization parameter [22,23], perform ECG signal processing [24], compute activation and repolarization times [13,15,16] etc. A recent review in the field summarizes these methods and puts them into perspective in terms of clinical applications [25]. Although our results may be generalizable to those methods, we did not investgate them in this study.

Conclusions

While there is qualitatively high visual consistency between the ECGI derived and recorded activation and repolarization maps, certain important features can be inaccurate, missing or artificial. These limitations arise due to a mismatch in reconstructed electrograms with a W-shaped QRS waveform, resulting in misplacement of activation markers in certain regions. By understanding these limitations, and extracting the features that are accurate, epicardial potential based ECGI can be effectively used in its current form as a useful clinical tool.

Acknowledgements

Conflict of interest: MC is part-time employed by Philips Research.

References

1. Leong KMW, Ng FS, Roney C, Cantwell C, Shun-Shin MJ, Linton NWF, et al. Repolarization abnormalities unmasked with exercise in sudden cardiac death survivors with structurally normal hearts. Journal of Cardiovascular Electrophysiology. 2018;29:115–26.

2. Zhang J, Sacher F, Hoffmayer K, O'Hara T, Strom M, Cuculich P, et al. Cardiac electrophysiological substrate underlying the ECG phenotype and electrogram abnormalities in brugada syndrome patients. Circulation. 2015;131:1950–9.

3. Andrews CM, Srinivasan NT, Rosmini S, Bulluck H, Orini M, Jenkins S, et al. Electrical and Structural Substrate of Arrhythmogenic Right Ventricular Cardiomyopathy Determined Using Noninvasive Electrocardiographic Imaging and Late Gadolinium Magnetic Resonance Imaging. Circulation: Arrhythmia and Electrophysiology. 2017;10.

4. Duchateau J, Sacher F, Pambrun T, Derval N, Chamorro-Servent J, Denis A, et al. Performance and limitations of noninvasive cardiac activation mapping. Heart Rhythm. 2018;

5. Oster HS, Taccardi B, Lux RL, Ershler PR, Rudy Y. Electrocardiographic imaging: Noninvasive characterization of intramural myocardial activation from inverse-reconstructed epicardial potentials and electrograms. Circulation. 1998;97:1496–507.

6. Wang Y, Rudy Y. Application of the method of fundamental solutions to potential-based inverse electrocardiography. Ann. Biomed. Eng. 2006;34:1272–88.

7. Bear LR, Huntjens PR, Walton R, Bernus O, Coronel R, Dubois R. Cardiac Electrical Dyssynchrony is Accurately Detected by Noninvasive Electrocardiographic Imaging. Heart Rhythm. Heart Rhythm Society; 2018;

8. Dallet C, Duchateau J, Hocini M, Bear L, Meo M, Sacher F, et al. Combined signal averaging and electrocardiographic imaging method to non-invasively identify atrial and ventricular tachycardia mechanisms. Computing in Cardiology Conference (CinC), 2016. 2016. p. 1–4.
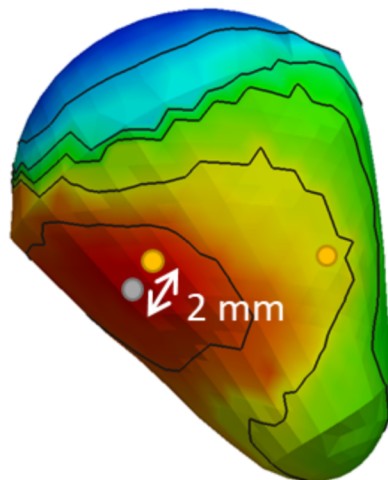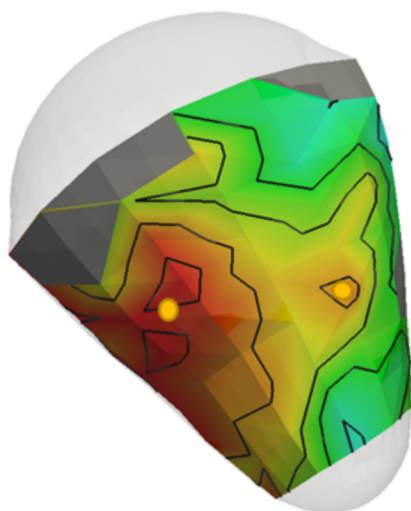
9. Tikhonov A, Arsenin V. Solution of ill-posed problems. Washington, D.C: John Wiley & Sons; 1977.

10. Colli-Franzone PC, Guerri L, Tentoni S, Viganotti C, Baruffi S, Spaggiari S, et al. A mathematical procedure for solving the inverse potential problem of electrocardiography. analysis of the time-space accuracy from in vitro experimental data☆ Mathematical Biosciences. 1985;77:353–96.

11. CIBC. Seg3D: Volumetric Image Segmentation and Visualization. Scientific Computing and Imaging Institute (SCI), Download from: http://www.seg3d.org. 2016.

12. Lux R, Gettes L. Repolarization heterogeneity and rate dependency in a canine rapid pacing model of heart failure. J Electrocardiol. 2011;44:730–5.

13. Duchateau J, Potse M, Dubois R. Spatially Coherent Activation Maps for Electrocardiographic Imaging. IEEE Transactions on Biomedical Engineering. 2016;64:1–8.

14. Rudy Y. Noninvasive imaging of cardiac electrophysiology and arrhythmia. Ann N Y Acad Sci. 2010;1188:214–21.

15. Erem B, Brooks DH, van Dam PM, Stinstra JG, MacLeod RS. Spatiotemporal estimation of activation times of fractionated ECGs on complex heart surfaces. Conference proceedings : Annual International Conference of the IEEE Engineering in Medicine and Biology Society. IEEE Engineering in Medicine and Biology Society. Annual Conference. 2011;5884–7.

16. Cluitmans MJM, Bonizzi P, Karel JMH, Das M, Kietselaer BLJH, de Jong MMJ, et al. In-Vivo Validation of Electrocardiographic Imaging. JACC: Clinical Electrophysiology. 2017;3:1–11.

17. He B, Li G, Zhang X. Noninvasive imaging of cardiac transmembrane potentials within three-dimensional myocardium by means of a realistic geometry anisotropic heart model. IEEE Transactions on Biomedical Engineering. 2003;50:1190–202.

18. Simms HDJ, Geselowitz DB. Computation of heart surface potentials using the surface source model. J Cardiovasc Electrophysiol. 1995;6:522–31.

1   19. van Oosterom A, Jacquemet V. A Parameterized Description of Transmembrane Potentials Used

2   in Forward and Inverse Procedures. Int Conf Electrocardiol. 2005;6:5–8.

3   20. Barr RC, Ramsey M, Spach MS. Relating epicardial to body surface potential distributions by

4   means of transfer coefficients based on geometry measurements. IEEE Trans. Biomed. Eng.

5   1977;24:1–11.

6   21. Bradley CP, Harris GM, Pullan AJ. The computational performance of a high-order coupled

7   FEM/BEM procedure in electropotential problems. IEEE Trans. Biomed. Eng. 2001;48:1238–50.

8   22. Karoui A, Bear L, Migerditichan P, Zemzemi N. Evaluation of fifteen algorithms for the resolution

9   of the electrocardiography imaging inverse problem using ex-vivo and in-silico data. Frontiers in

10 Physiology. 2018;9.

11 23. Barnes JP, Johnston PR. Application of robust Generalised Cross-Validation to the inverse

12 problem of electrocardiology. Computers in biology and medicine. 2016;69:213–25.

13 24. Bear LR, Dogrusoz YS, Svehlikova J, Good W, Dam E Van, Macleod R, et al. Effects of ECG Signal

14 Processing on the Inverse Problem of Electrocardiography. Computing in Cardiology. 2018;5–8.

15 25. Cluitmans M, Brooks D, MacLeod RS, Doessel O, Guillem M, Van Dam P, et al. Consensus on

16 validation and opportunities of electrocardiographic imaging: From technical achievements to clinical

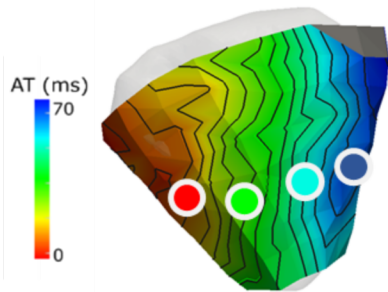17 applications. Frontiers in Physiology [Internet]. 2018;9:1305. Available from:

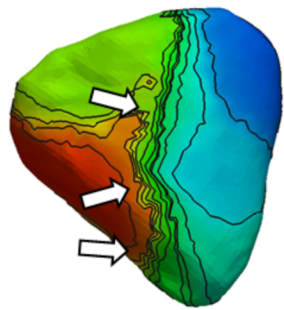18 https://www.frontiersin.org/articles/10.3389/fphys.2018.01305/abstract
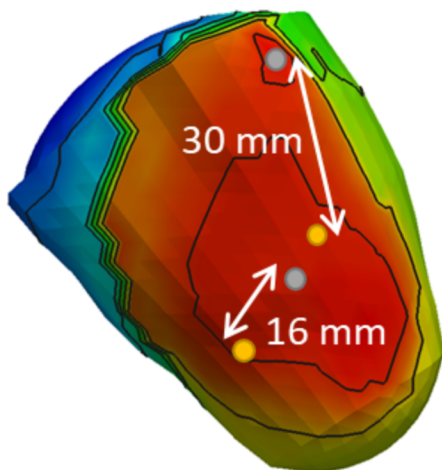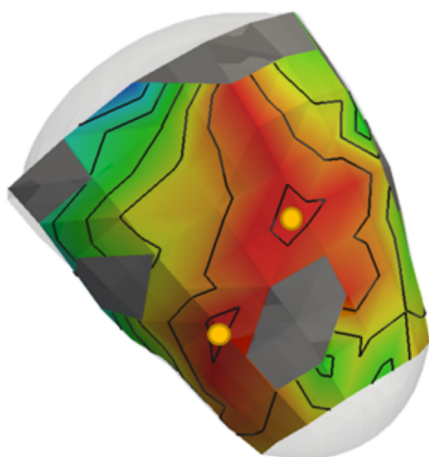
19

Recorded | ECGI

(a)

AT (ms)
70
0

2 mm

(b)

AT (ms)
75
0

30 mm

16 mm

(a) Recorded — ECGI (mdVdT, Spatiotemporal)

AT (ms)
70
0

(b) Recorded

(c) ECGI

(d)
***

No Line of Block   Line of Block

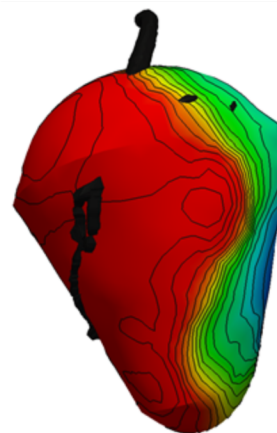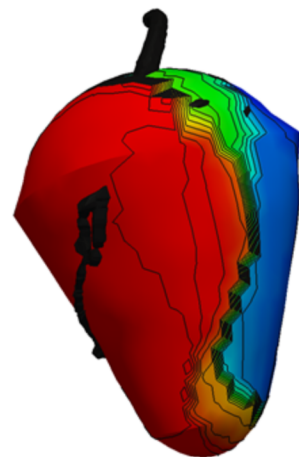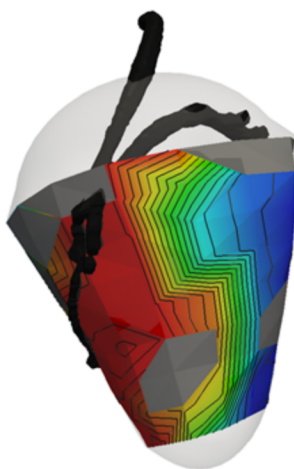| Recorded	ECGI	
	mdVdT	Spatiotemporal

(a)

(b)

RT (ms)

310

180
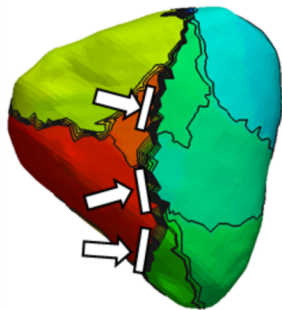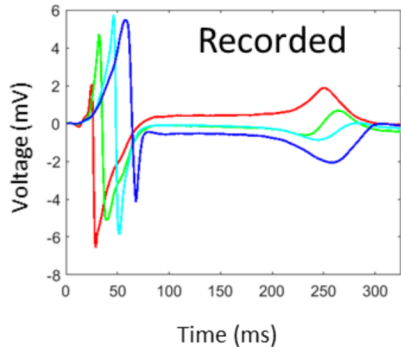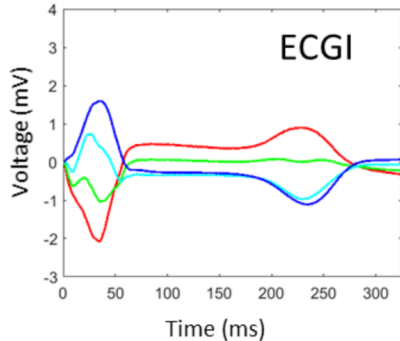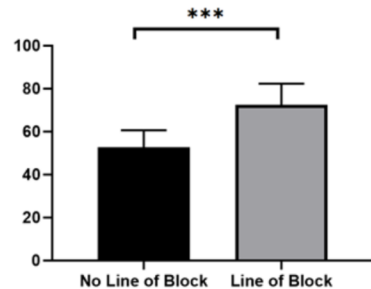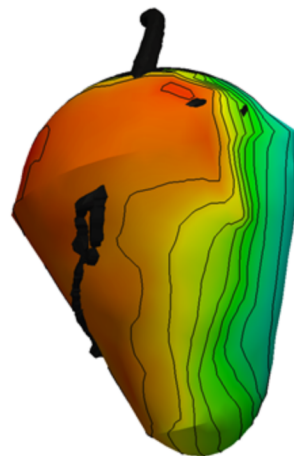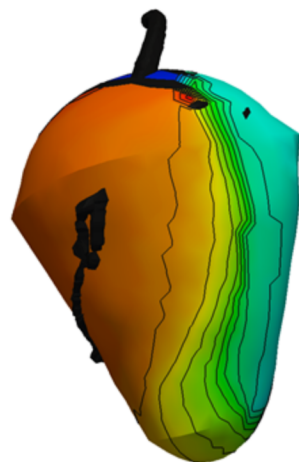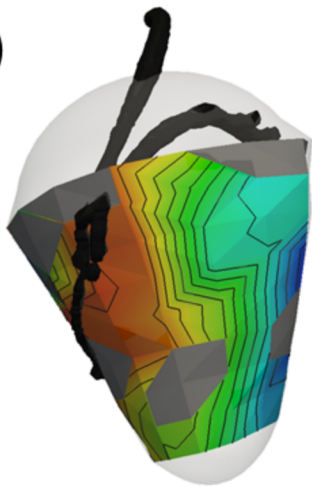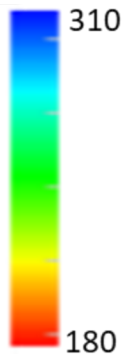
Table 1: The mean absolute error (MAE) and the correlation coefficient (CC) between recorded and ECGI reconstructed activation and repolarizations maps. Activation and repolarization times were computed from ECGI reconstructed signals using either the min/max mdV/dt method or a spatio-temporal approach. Difference between spatio-temporal and dV/dt results (*p<0.01; **p<0.001); Difference between recovery and activation results using the same marker method (†p<0.01; ††p<0.001).

		MAE (MS)	**CC**
ACTIVATION	min dV/dt	8.4 ± 4.5	0.68 ± 0.13
	spatio-temporal	7.5 ± 4.3**	0.75 ± 0.13**
REPOLARIZATION	max dV/dt	28 ± 11††	0.64 ± 0.16
	spatio-temporal	31 ± 10*††	0.60 ± 0.19†

1   *Table 2: Comparison of specific features in activation and repolarization maps. Activation times were*

2   *computed from ECGI reconstructed signals using a spatio-temporal approach, and repolarization times*

3   *using max mdV/dt.*

		LOCALIZATION ERROR (MM)	OFFSET TIMING (MS)	SIZE DIFFERENCE (MM^2)
ACTIVATION	Epicardial Breakthroughs	22.3 ± 18.5	1.6 ± 1.4	-
REPOLARIZATION	Early Abnormal Region	2.6 ± 2.1	3.4 ± 4.4	-76 ± 112
	Late Abnormal Region	2.2 ± 2.6	7.3 ± 3.0	70 ± 53

4

5

6